Modified embedded atom method potential for Fe-Al intermetallics mechanical strength: A comparative analysis of atomistic simulations

Muhammad Zeeshan Khalid [a,b,*], Jesper Friis [c,d], Per Harald Ninive [a], Knut Marthinsen [b], Inga Gudem Ringdalen [c], Are Strandlie [a]

[a] *Department of Manufacturing and Civil Engineering, Norwegian University of Science and Technology, Gjøvik, 2815, Norway*
[b] *Department of Materials Science and Engineering, Norwegian University of Science and Technology (NTNU), Norway*
[c] *SINTEF Materials and Chemistry, Trondheim, Norway*
[d] *Department of Physics, Norwegian University of Science and Technology, Trondheim, Norway*

A B S T R A C T

The structural and mechanical properties of Fe-Al compounds ($FeAl$, Fe_2Al, Fe_3Al, $FeAl_2$, $FeAl_3$, Fe_2Al_5) have been studied using modified embedded atom method (MEAM) potentials. The equilibrium lattice constants, formation enthalpies, and elastic properties have been investigated and compared with other studies. The calculated lattice constants show good agreement with the embedded atom method (EAM) and density functional theory (DFT) calculations and with experiments. All Fe-Al compounds are mechanically stable according to the elastic constants restrictions. The calculated bulk modulus of the compounds does not show a linear relation with Fe concentration, which is most probably caused by the mechanical anisotropy of Fe-Al compounds. However, comparison of the Fe-Al mechanical properties of MEAM, DFT and EAM-based approaches and experiments show non-consistent differences, which reflects uncertainties with several of these methods, due to assumptions and simplifications imposed during calculations. In general, DFT calculations are closer to experimental observations than semi-empirical potentials. Comprehensive comparisons are made based on theoretical and experimental methodologies.

1. Introduction

Fe-Al compounds have been gaining a lot of attention due to their increased industrial interest owing to the light-weight, corrosion resistance and high-temperature resistance behavior [1–3]. FeAl compounds including Fe_3Al, $FeAl$, Fe_2Al_5, $FeAl_2$ and $FeAl_3$ have been the main focus of research in many different industrial areas, for example, high-temperature structural materials, composite materials, protective coatings for materials and functional materials. Fe-Al materials have been considered very promising because they are considered as potential candidates for replacing steel [4,5].

Many researchers have performed atomistic simulations to predict the mechanical strength of Fe-Al compounds [6–10]. Zhang et al. [6] studied the structural and mechanical properties of these compounds by EAM simulations. Liu et al. [10] studied the mechanical and electronic properties of Fe-Al compounds by an ab-initio method. Jelinek et al. [9] developed the MEAM and calculated the lattice constants, formation enthalpy and bulk modulus of $FeAl_3$, $FeAl_2$, $FeAl$, and Fe_3Al compounds. Liu et al. [11] studied the FeAl compound and calculated the elastic properties from first-principles calculations. Niu et al. [12]

performed first-principles simulations for the prediction of mechanical properties and electronic structure of the Fe_3Al compound.

All these simulations were performed on a single unit cell of Fe-Al compounds without considering any crystal defects. However, results from simulations have shown contrasting trends about the mechanical properties of these compounds. The differences can be caused by the following reasons, (i) the mechanical properties change at higher temperatures, (ii) the potentials used for calculations are inaccurate and require further improvements. To signify the differences between different semi-empirical potentials and first-principles studies, we have made comparisons of mechanical properties of Fe-Al compounds with experiments. We also studied the inaccuracy of these atomistic simulations, and tried to find the best atomistic methodology for the prediction of actual trends about Fe-Al compounds.

In this paper, we have investigated the structural and mechanical properties of Fe-Al compounds ($FeAl$, Fe_2Al, Fe_3Al, $FeAl_3$, Fe_2Al_5) analyzed by semi-empirical interatomic potentials, i.e. the MEAM method [9,13]. MEAM is extensively applied for metallic systems [14–16] and it agrees reasonably well with experiments [17,18]. The MEAM

* Corresponding author at: Department of Materials Science and Engineering, Norwegian University of Science and Technology (NTNU), Norway.
  E-mail address: muhammad.z.khalid@ntnu.no (M.Z. Khalid).

potential mono-atomic parameters fitted to Al and Fe and their binary combination developed by Jelinek et al. [9] are used in this study. Other studies have already reported the structural properties of Fe-Al compounds by using the MEAM potentials. In this study, however, we are exploring the mechanical properties of Fe-Al compounds and discuss the reliability and applicability of semi-empirical potentials for extracting actual values by comparing it with density functional theory (DFT) and experiments.

2. Method of calculation

2.1. Interatomic potential

In DFT, the electron structure of a many-electron systems is solved, which is computationally very intensive. For this reason, a direct numerical solution can only be applied to smaller systems so far. To overcome this limitation, molecular dynamic (MD) simulations offer an opportunity of studying larger systems. In MD, the interaction between atoms is described by Newton's classical equation of motion, which in the simplest form for a particle of mass m_i ($i = 1, 2, \ldots, N$) with interaction potential Φ, can be defined as [19]:

$$\vec{F}_i = m_i \frac{d^2}{dt^2} \vec{r}_i = -\nabla_i \Phi(\vec{r}_i - \vec{r}) \tag{1}$$

where $\nabla_i \Phi$ is the force field felt by the atom i, $\vec{r}_i$ is the position of atom i and $\vec{r}$ is the mass center of system. To describe the interatomic interaction, many researchers have developed empirical and semi-empirical interatomic potentials, whose parameters are mainly determined by results from density functional theory.

MD simulations frequently approximate the atomic interaction with an average interaction from neighboring atoms. One of the most common and widely used interatomic potentials is the embedded atom method (EAM) developed by Baskes [20], which consider many-body terms suitable for metallic systems.

The modified EAM (MEAM) method is a generalization of EAM that in addition includes (i) the directional bonding effect and (ii) a screening function is introduced to limit the number of interactions between the atoms. Even with the introduction of new parameters, the MEAM potentials struggle to predict experimentally consistent results for BCC metals [14,15]. For example, MEAM has predicted that other metals are thermodynamically more stable than BCC metals, while it is experimentally well known that BCC metals are more stable [14,15]. Moreover, surface energies of low-index surfaces of BCC metals are not consistent with experiments. This failure of the MEAM potentials for BCC is assumed to be caused by the fact that only nearest-neighbor interactions are considered. To overcome this shortcoming, second-nearest neighbor interactions (2NN) have been introduced by adjusting the screening parameter [21]. The MEAM formalism is thoroughly described in literature [16,21,22].

2.2. MEAM parameters and simulation technique

The MEAM parameters used in this work for Al and Fe are given in Table 1. The initial values were directly taken from MEAM potentials [16,22] without any modifications. E_c and a_0 depends on the material properties (see Table 1 caption), if the initial reference structure is known. It is either directly taken from the experiments or optimization of the structure. The other important parameter is C_{min}, which defines the extent of screening of an atom (k) with the neighboring atoms (i and j). The elements are the same for pure elements (i-j-k=A-A-A or B-B-B), however for Fe-Al compounds, one of the screening atoms could be different (i-j-k=A-B-A, B-A-B, A-A-B, B-B-A) [23]. For this reason a different value of C_{min} has to be assigned. To improve the generalized stacking fault energy curves, the value of C_{min} was reduced to 0.8 from 2 for Al [9]. C_{max} has been given a fixed value of 2.8 for Fe and 1.9 for Al. C_{max} determines the position of an

atom (k) that begins screening with a second neighboring atom (i or j). The values of C_{min} and C_{max} thereby define the range of screening to nearest-neighbor interactions. The density scaling factor ρ_0 also affects the calculations. For pure elements, the factor has been removed, but for alloys and compounds with different types of elements, this factor may have a great effect on the calculations.

The parameters listed in Table 1 are determined by fitting the experiments or by density functional theory based calculated physical properties for Fe-Al binary compounds. The MEAM parameters for Fe-Al compounds were initialized to match the DFT-calculated heat of formation, bulk modulus, equilibrium volume and elastic moduli to the hypothetical NaCl reference structure [9]. NaCl was chosen as a reference structure due to its direct relevance with MEAM and simplicity. Based on a trial and error method, parameters were varied until the properties calculated showed good agreement with DFT and experimental values. Those values were then further considered for Fe-Al compounds and shown in Table 1. The most important parameter which affects the physical properties of the compounds is the density scaling factor ρ_0 for the element pair. For Fe-Al binary compounds, it is selected to be 1 [9]. The remaining parameters β^n and t^n ($(n = 1, 2, 3)$) are adjustable parameters, and values are determined by the fitting of physical properties with DFT.

After the selection of suitable values for MEAM parameters, the simulations were run by using an Atomistix Toolkit (ATK) forcefield [24,25]. Before the calculations of elastic constants, the geometry of the material was optimized by relaxing the atoms until the maximum forces and stresses were less than 0.001 eV/atom and 0.01 GPa, respectively. To obtain the equilibrium structure of Fe-Al intermetallics, the quasi-Newton optimizer "Limited-memory Broyden–Fletcher–Goldfarb–Shanno (LBFGS)"[26] was adopted.

2.3. Calculations of elastic constants

The elastic constants are related to the various components of stress and strain by:

$$\sigma_{ijl} = C_{ijk} \epsilon_{kl} \tag{2}$$

where σ_{ijl}, C_{ijk} and ϵ_{kl} are the stress, elastic components and strain tensor, respectively. After the calculations of elastic constants, various mechanical properties of Fe-Al compounds such as, bulk modulus (B), Young's modulus (Y), shear modulus (G) and Poisson's ratio (v) can be obtained by using the Voigt–Reuss–Hill (VRH) approximation [27–29]. The bulk modulus (B) and shear modulus were obtained by Eq. (3) and (4), respectively, and the VRH approximation was used to calculate the average of the lower and upper bounds of the elastic modulus. Young's modulus (Y) and Poisson's ratio (v) were calculated from the bulk modulus and shear modulus by using Eq. (5)–(6) (for cubic systems).

$$B = [2(C_{11} + C_{12} + 2C_{13}) + C_{33}]/9 \tag{3}$$

$$G = (7C_{11} - 5C_{12} + 2C_{33} + 12C_{44} - 4C_{13})/30 \tag{4}$$

$$Y = 9BG/(3B + G) \tag{5}$$

$$v = (3B - 2G)/2(3B + G) \tag{6}$$

The mechanical stability of these compounds has also been studied in this paper. The elastic stability criteria in various crystal structure systems can be found in Appendix.

3. Results and discussions

3.1. Structural properties

MEAM potentials were used to calculate equilibrium lattice constants, equilibrium volume, and formation enthalpy as shown in Table 2. Calculated structural values are compared with available experimental results, interatomic potentials, and DFT studies. As can be

Table 1
Set of MEAM parameters for fcc Al and bcc Fe. E_c is the cohesive energy, a_0 is the equilibrium lattice constant, A is the scaling factor for embedding energy. α is exponential decay factor for the universal energy, β^{0-3} are the exponential decay factors for the atomic energies, t^{0-3} are the weighting factors for the atomic densities, C_{max} and C_{min} are the screening parameters, and ρ_0 is the density scaling factor relevant for the element pairs.

Element	E_c(eV)	a_0(∀)	A	α	β^0	β^1	β^2	β^3	t^0	t^1	t^2	t^3	C_{min}	C_{max}	ρ_0
Al	3.35	4.04	1.07	4.64	2.04	3.0	6.0	1.5	1.0	4.5	−2.3	8.01	0.8	2.8	1.0
Fe	4.28	2.851	0.55	5.027	3.5	2.0	1.0	1.0	1.0	−1.6	12.5	−1.4	0.68	1.9	1.0

Table 2
The calculated lattice parameters from the present calculations compared with references and measured values. H_f is the formation enthalpy and V_0 is the equilibrium volume per atom calculated in Å^3.

Phase	Space group	Species	a_0(Å)	b_0(Å)	c_0(Å)	V_0 (Å^3)	H_f(eV/atom)
FeAl	Pm3m	This work	2.953	-	-	12.87	−1.48
		EAM/MEAM	2.893 [6]	-	-	12.88 [9]	−1.42 [33]
		DFT [10]	2.851 [10]	-	-	12.07	−0.390 [10]
		Exp.	2.909 [30]	-	-	[31]	−0.423 [34]
		Exp.	-			12.23 [32]	−0.28 [35]
						-	
Fe$_3$Al	Fm3m	This work	5.769			12.00	−0.53
		EAM/MEAM	5.764 [6]			12.01 [9]	−0.279 [6]
		DFT	5.586 [10]			12.01	−0.217 [10]
		Exp.	5.789 [36]			[31]	−0.202 [37]
		Exp.	5.792 [30]			12.07 [32]	−0.321 [34]
						-	
FeAl$_3$	C2/m	This work	16.680	7.860	12.220	15.73	−0.532
		EAM/MEAM	15.069 [6]	7.864	12.083	15.03 [9]	−0.059 [6]
		DFT	15.352 [10]	8.010	12.398	13.91 [9]	−3.923 [10]
		DFT	15.125 [7]	4.012 [7]	11.839	-	−4.562 [7]
		Exp.	15.49 [30]	8.08	[7] 12.48	-	n.a
FeAl$_2$	P1	This work	4.054	6.687	8.802	15.77	−0.093
		EAM/MEAM	4.6212 [6]	6.372	8.629	14.71 [9]	−0.160 [6], −0.076 [9]
		DFT	4.793 [10]	6.351	8.658	12.78 [9]	−0.286 [10]
		Exp.	4.787 [30]	4.787	6.461	-	n.a
Fe$_2$Al$_5$	Cmcm	This work	7.462	6.717	4.464	15.96	−1.0303
		EAM	7.622 [6]	6.323	4.178		−0.146 [6]
		DFT	7.466 [10]	6.181	4.808		−8.385 [10], 7.352 [7]
		Exp.	7.675 [30]	6.403	4.203		n.a

seen, the calculated lattice constants of FeAl from MEAM potentials are consistent with experimental studies [30,36]. The results are as good as DFT and somewhat inferior to EAM. The calculated formation enthalpy for FeAl is −1.49 eV/atom, which is consistent with EAM [6] studies (−1.42 eV/atom). However, DFT results from [10] have shown better agreement with experiments as compared to EAM/MEAM potentials. We applied this potential for other Fe-Al IMCs as well. For another cubic structure, Fe$_3$Al (Fm3m), our calculated lattice constants are larger than those reported in other theoretical studies [6,10], but shows better agreement with experimental values [30,36]. For the monoclinic structure FeAl$_3$, the differences between lattice constants are found to be largest along the a_0 unit direction with a 7.68% difference to experimental values [30]. For the orthorhombic Fe$_2$Al$_5$ and trigonal FeAl$_2$ structures, the difference between lattice constants was found to be 2.77-6.20% and 15.31% along a, b and c lattice directions, respectively. These differences to experimental values indicate that the MEAM potentials are inaccurate and do not describe well low symmetry structures. EAM potentials [6] have also shown this tendency. The reason for this inaccuracy is attributed to the background electron density. In MEAM and EAM potentials, the background electron density is used to describe the many-body interactions and is assumed to be a homogeneous electron gas [6]. This may well describe high-symmetry structures such as a cubic structure, but it is not obvious that it describes the directional effects in low symmetry structures equally well.

We calculated the formation enthalpies by studying the energies of the optimized structures for the Fe-Al compounds as given in Table 2. All calculated values were compared with other theoretical [6,10,33]

and experimental [34,35,37] results and plotted in the graph shown in Fig. 1. It is generally accepted that the stability of a compound can be predicted by the values of formation enthalpies. Based on our calculations, all Fe-Al compounds have negative formation enthalpies, showing that they are thermodynamically stable. For cubic structures (FeAl, Fe$_3$Al), the formation enthalpies were found to be higher for all theoretical studies as compared to experiments, but for low-symmetry structures (FeAl$_3$, Fe$_2$Al$_5$ and FeAl$_2$) the opposite is found. Based on MEAM calculations, FeAl has the highest negative value (−1.48 eV/atom)) among the Fe-Al compounds, hence it is deemed to be thermodynamically more stable than any other Fe-Al compound studied in this work. This conclusion is consistent with EAM [6] studies, but contradicts with DFT results [10], which predicts Fe$_2$Al$_5$ to be the most stable compound.

3.2. Elastic constants and mechanical properties

In this section, we are investigating the elastic constants and mechanical strength of the different Fe-Al compounds. Table 3 lists the calculated elastic constants compared with EAM [6], DFT [10], long-range analytical embedded atom method (LAEAM) [38], and experimental studies [37,39]. It is well known that different symmetries impose different constraints on the elastic constants. These constraints are defined from A.2-A.4 (see Appendix) for the cubic, orthorhombic, monoclinic and trigonal systems. Elastic constants calculated for FeAl (cubic), Fe$_3$Al (cubic), FeAl$_3$ (monoclinic), FeAl$_2$ (trigonal) and Fe$_2$Al$_5$ comply with the respective restriction criteria, which implies that these compounds are mechanically stable.
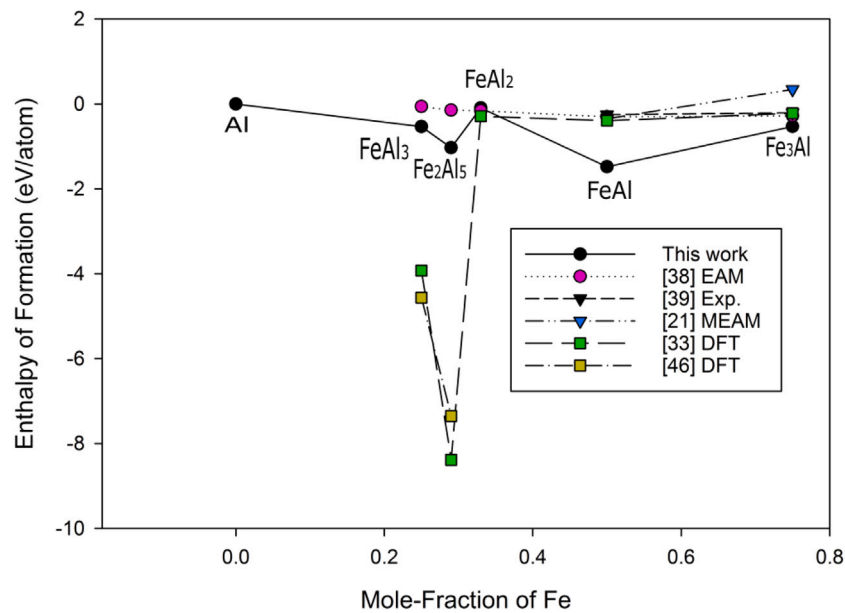
Fig. 1. Comparison of calculated formation enthalpies of Fe-Al compounds with other studies.

Table 3
Elastic constants (in GPa).

Comp.	Method	C_{11}	C_{12}	C_{13}	C_{22}	C_{23}	C_{33}	C_{44}	C_{55}	C_{66}	C_{14}	C_{15}	C_{25}	C_{35}
FeAl Pm3m	This work	256.26	94.96					115.88						
	EAM [6]	179.1	132.9					116.6						
	DFT [10]	294.0	133.7					157.0						
	LAEAM [38]	224.6	146.6					113.6						
		251.4	92.2					111.7						
	MEAM [9]	207.7	121.4					126.2						
	Exp. [37]	181.1	113.7					127.1						
	Exp. [39]													
Fe$_3$Al Fm3m	This work	188.51	125.34					121.65						
	EAM [6]	187.9	133.3					138.1						
	DFT [10]	284.7	207.5					151.0						
	LEAM [38]	212.5	160.2					124.8						
	MEAM [9]	177.5	117.5					129.0						
	Exp. [39]	171.0	130.6					131.7						
FeAl$_3$ C2/m	This work	148.91	60.26	46.80	147.42	56.64	160.35	45.77	58.75	13.77		-5.12	4.25	-5.86
	EAM [6]	168.5	80.3	72.8	148.2	72.9	182.0	−17.2	25.1	34.2		3.9	9.1	−7.1
	DFT [10]	248.9	71.8	67.6	260.2	49.5	259.6	76.1	65.4	109.6				
FeAl$_2$ Pl	This work	172.34	37.29	49.79	141.92	62.64	158.71	51.87	67.43	38.09	19.22			
	EAM [6]	223.9	71.5	88.1	194.5	101.0	184.4	81.6	68.6	52.3	−12.0			
	DFT [10]	223.3	88.3	77.4	260.7	78.2	263.1	94.1	89.1	92.8				
Fe$_2$Al$_5$ Cmcm	This work	205.58	28.89	52.09	123.99	81.52	103.29	36.70	47.40	53.61				
	EAM [6]	126.0	136.2	71.8	97.4	49.2	174.1	13.8	21.6	18.2				
	DFT [10]	294.4	68.4	45.6	300.4	60.0	256.3	109.6	97.7	84.5				

As given in Table 3, good agreement was found with experimental studies for cubic structures (FeAl, Fe$_3$Al). FeAl elastic constants were found to be slightly overestimated compared with experimental studies [37,39] but underestimated when compared with DFT results in [40]. The same conclusion can be drawn for other crystal structures. Overall DFT [7,10] elastic constants show higher values when compared with EAM [6], LAEAM [38] and MEAM [8,9].

To better understand the mechanical strength of Fe-Al compounds, mechanical properties such as bulk modulus, shear modulus, Young's modulus, and Poisson's ratio were calculated from the elastic constants. Table 4 lists the calculated values for the relevant Fe-Al compounds. Our calculated bulk modulus is similar to the experimental bulk modulus [39] for the FeAl compound and closer to the experimental result than any of the other theoretical studies [6,8,9,38]. To make comparisons and interpret the results, bulk moduli of the Fe-Al compounds with different amount of Fe are plotted in Fig. 2. The differences to

other studies and experimental values reported in this study may be attributed to the following reasons: (i) defects in the crystal structures were ignored, and (ii) effects of anisotropy on the elastic constants are not considered. As shown in Fig. 2, with increasing contents of Fe, the bulk modulus decreases from FeAl$_3$ to FeAl$_2$, but for FeAl (138.3 GPa) and Fe$_3$Al (123.99 GPa) it again shows an increase. Since bulk Fe has a higher bulk modulus than Al, the bulk modulus is expected to increase with an increase in the Fe concentrations. However, the anisotropy of the crystal could affect this trend. To visualize the anisotropic properties we plotted 3D plots of directional dependencies of Young's modulus (see Fig. 3) using spherical coordinates. Readers are referred to the following Refs. [40,44] for details on the theoretical construction of anisotropic behavior of isotropic crystal structures. As shown in Fig. 3 the least anisotropic structure is FeAl with the highest values of Young's modulus along the <111> direction, while Fe$_3$Al is found to be the most anisotropic structure. For this reason, FeAl shows a higher bulk modulus value despite having a lower Fe content as compared to

Table 4
The calculated bulk modulus (B), shear modulus (G), Young's modulus (Y) and Poison's ratio (v) of Fe-Al compounds.

| Comp.	Method	B (GPa)	G (GPa)	Y (GPa)	B/G	v
FeAl Pm3m	This work	138.3	103.03	247.61	1.34	0.20
	EAM [6]	148.2	55.9	148.9	2.65	0.33
	MEAM [8]	124.5	-	-	-	-
	MEAM [9]	145.3	-	-	-	-
	DFT [10]	187.1	119.8	296.2	1.56	0.236
	Exp. [39]	136.1	-	-	-	-
Fe$_3$Al Fm3m	This work	123.99	72.572	182.17	1.71	0.255
	EAM [6]	151.5	66.2	173.4	2.29	0.309
	MEAM [8]	148.9	-	-	-	-
	MEAM [9]	137.5	-	-	-	-
	DFT [10]	233.2	87.9	234.0	2.65	0.33
	Exp. [39]	144.1	-	-	-	-
FeAl$_3$ C2/m	This work	87.047	37.88	99.23	2.30	0.31
	EAM [6]	105.6	23.80	65.9	4.44	0.376
	MEAM [9]	103.5	-	-	-	-
	DFT [10]	127.3	89.7	232.1	1.42	0.215
	DFT [7]	94.41	76.65	218.0	1.23	0.185
FeAl$_2$ P1	This work	83.836	49.51	124.09	1.69	0.25
	EAM [6]	124.90	49.8	47.0	2.51	0.32
	MEAM [9]	90.4	-	-	-	-
	DFT [10]	136.5	87.8	216.9	1.55	0.235
Fe$_2$Al$_5$ Cmcm	This work	85.53	39.502	102.37	2.17	0.295
	EAM [6]	101.3	16.5	47.0	6.14	0.423
	DFT [10]	127.5	97.0	232.1	1.31	0.196
	DFT [7]	126.92	85.84	210.16	1.48	0.224
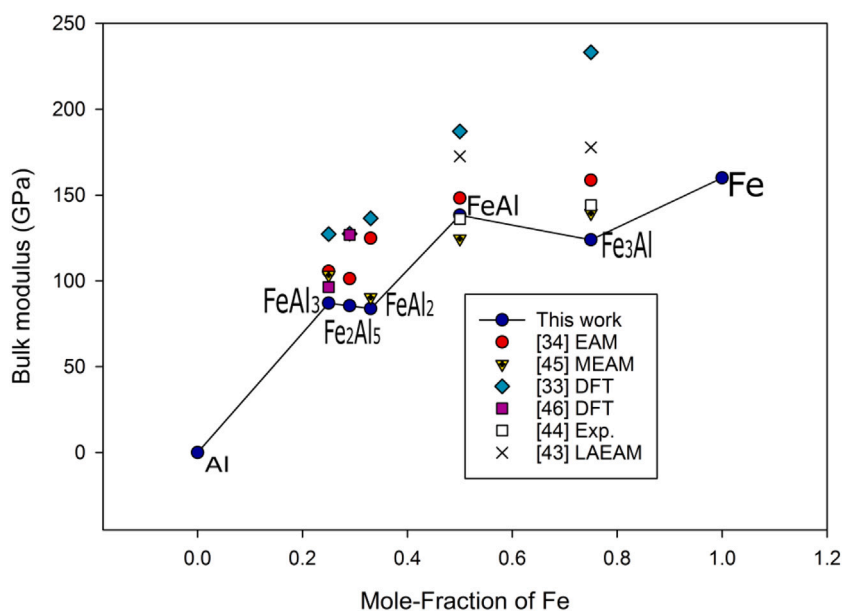
Fig. 2. Comparison of calculated bulk modulus with previous studies.

Fe$_3$Al. Moreover we can clearly see that Fe$_2$Al$_5$ is more anisotropic than FeAl$_3$ and FeAl$_2$. This shows that the material's mechanical properties are largely influenced by the anisotropic nature, which is why we see different trends in the bulk modulus with varying contents of Fe (Fig. 2).

Haines et al. [45] showed that materials with higher shear and Young's modulus have a tendency of showing a higher hardness [46, 47]. Therefore FeAl, which is found to be the material with the largest moduli ($G = 103.03$ GPa, $Y = 247.61$ GPa) is a hard phase, while FeAl$_3$ with the smaller moduli ($G = 37.88$ GPa, $Y = 99.23$ GPa) is a softer phase. Poisson's ratio can provide important information about the brittle and ductile nature of the material. It is generally accepted that materials with low Poisson's ratio are brittle [48,49]. From Table 4, we can see that FeAl has the lowest Poisson's ratio value, which indicates a brittle nature of FeAl.

To obtain further insight into the brittle and ductile nature of compounds, an empirical criterion of fracture has been proposed [50]. According to this criterion, the ratio between the bulk modulus (B) and the shear modulus (G) provides important information about the brittle and ductile nature of relevant compounds. Materials having $B/G > 1.75$ are assumed to be ductile, while materials having a ratio smaller than this are expected to exhibit brittle properties. From Table 4 we can see that FeAl, Fe$_3$Al and FeAl$_2$ have $B/G < 1.75$, which indicates that these materials are brittle. When comparing to different methodologies in literature, we have found a mixed trend for the properties of the Fe-Al IMCs. Based on the available data on the mechanical properties, Table 5 shows the ambiguity about certain property predictions of the Fe-Al compounds based on different theoretical and experimental methods.
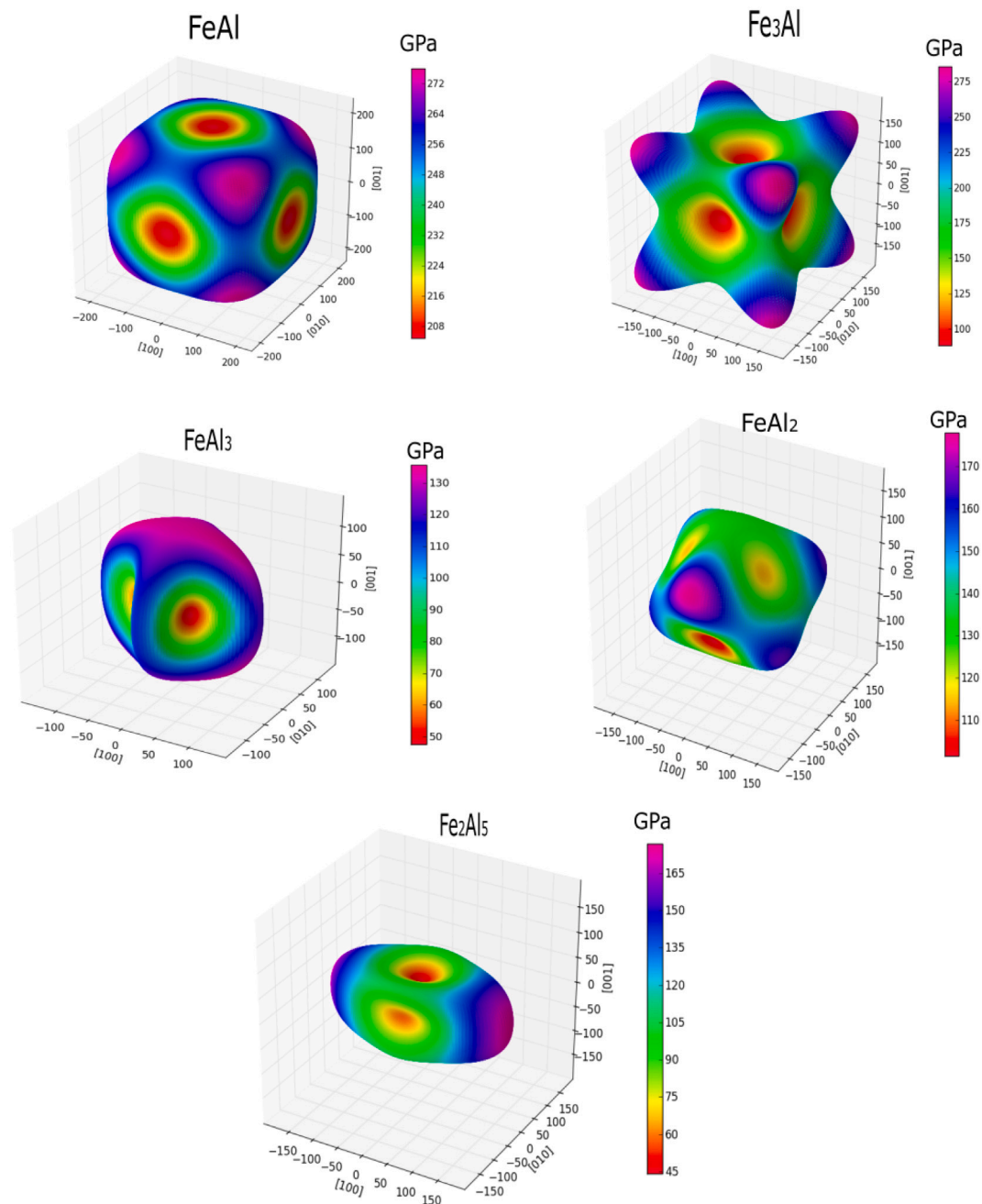
Fig. 3. Directional dependence of Young's modulus of different Fe-Al compounds. The visualization is generated using the SC-EMA software package (freely available at http://scema.mpie.de) [41–43].

The compressibility of a compound can be related to the bulk modulus of the material. Materials having higher bulk modulus are more resistant to compression. We find FeAl as the most resistant to compression, with the highest bulk modulus. By comparing our calculated values with other available literature, we find some discrepancies with respect to this property. This work is in good agreement with other studies performed using MEAM potentials [9], but differs from EAM [6], DFT [10] and experimental studies [39]. In terms of the brittle and ductile nature of these compounds, an EAM study found [6] that all compounds are ductile, which does not fit well with DFT [10] and our work. Furthermore, many experimental studies have reported the brittle nature of these Fe-Al compounds, particularly Fe_2Al_5 and $FeAl_3$ [51]. Both MEAM (this work) and EAM [6] are unable to predict precisely the brittle nature of Fe_2Al_5 and $FeAl_3$ compounds, while DFT studies [7,10] have shown good agreement with experimental observations. In terms of hardness of these compounds, this work predicted FeAl as the hardest phase, which agrees well with DFT but contradicts with EAM and experiments. A good agreement is also found with DFT in terms of mechanical anisotropy predictions of these compounds. This work shows agreement with experiments in predicting $FeAl_3$ as a soft phase. Hardness reported in experimental studies is dependent on the temperature range, welding or experimental methodologies. Since the present simulations were performed without considering temperature, deviations from experiments are inevitable.

Table 5
Difference in mechanical properties of Fe-Al compounds reported in literature. All properties are described in descending order.

Property	This work	EAM [6]	MEAM [9]	DFT [10]	Exp. [39,51,52]
Compressibility	$FeAl>Fe_3Al>$ $FeAl_3>Fe_2Al_5>$ $FeAl_2$	$Fe_3Al>FeAl>$ $FeAl_2>FeAl_3>$ Fe_2Al_5	$FeAl>Fe_3Al>$ $FeAl_3>FeAl_2$	$Fe_3Al>FeAl>$ $FeAl_2>Fe_2Al_5>$ $FeAl_3$	$Fe_3Al>FeAl$
Brittle to ductile	$FeAl$ (brittle)$>FeAl_2$(brittle)$>$ Fe_3Al (brittle)$>$ Fe_2Al_5(ductile)$>FeAl_3$(ductile)	All compounds Ductile	Not reported	Fe_2Al_5 (brittle)$>$ $FeAl_3$(brittle)$>$ $FeAl_2$ (brittle)$>$ $FeAl$(brittle)$>Fe_3Al$(ductile)	Brittle phases Fe_2Al_5 $FeAl_3$
Hardness and stiffness	$FeAl>Fe_3Al>$ $FeAl_2>Fe_2Al_5>$ $FeAl_3$	$Fe_3Al>FeAl>$ $FeAl_2>FeAl_3>$ Fe_2Al_5	–	$FeAl>Fe_2Al_5>$ $Fe_3Al>FeAl_3>$ $FeAl_2$	$Fe_3Al>FeAl$ $Fe_2Al_5>FeAl_2$ $FeAl_3$ $FeAl>FeAl_3>FeAl_2$ $>Fe_2Al_5$
Mechanical anisotropy	$Fe_3Al>Fe_2Al_5>$ $FeAl_3>FeAl_2>FeAl$	Not Reported	–	$Fe_3Al>FeAl>$ $Fe_2Al_5>$ $FeAl_2>FeAl_3$	

4. Discussion

We have performed MEAM simulations and made comparisons of interatomic potentials with experiments and DFT. It is hard to find a perfect match with experiments due to the simplifications and generalizations imposed during computational calculations, but general trends can still be extracted as indications of actual properties. All these single-crystal simulations are performed without considering crystal defects, hence the values calculated from these calculations are over-estimated as compared to the experimental values. Still, these calculations provide vital insights into the mechanical behavior of ideal compounds. In this study, we have made comparisons of the Fe-Al compounds with other simulation techniques and methods. To be consistent in our comparisons, we only considered single-crystal calculations without any crystal defects.

Table 5 shows comparisons of the materials mechanical properties based on the calculated elastic constants. As discussed in Section 3, there are contrasting differences between the mechanical properties of these compounds. When compared to the available experimentally reported mechanical behavior of these compounds, it has been generally accepted that Fe_2Al_5 and $FeAl_3$ are brittle intermetallic compounds. However, semi-empirical potentials such as EAM and MEAM are unable to predict the brittle nature of these compounds. There are several plausible explanations for this observation: (i) these compounds are ductile at lower temperature and turn brittle at higher temperatures, (ii) crystal defects such as cracks and impurities significantly alter the mechanical properties of these compounds, and (iii) these potentials are inaccurate and not able to predict actual properties. Despite the first two assumptions, DFT calculations successfully predict the brittle nature of Fe_2Al_5 and $FeAl_3$ compounds. This shows that the interatomic potentials are not accurate enough in predicting the mechanical properties of low symmetry structures.

Furthermore, calculations of bulk modulus, shear modulus and Young's modulus from first-principles showed significantly higher values as compared to semi-empirical potentials. For the case of FeAl and Fe_3Al compounds, the bulk modulus calculated by EAM and MEAM are closer to the experimental value than the value from DFT (Table 4). It is worth mentioning that numerous experimental values also implicitly constitute contributions from crystal defects. For this reason, values calculated from single crystal calculations are over-estimated as compared to the experimental values. DFT calculations significantly over-estimate bulk modulus values compared to the experimental values, due to a too idealistic modeling of FeAl and Fe_3Al compounds.

5. Conclusions

In this paper, structural and mechanical properties of different Fe-Al compounds were investigated using the MEAM. The calculated values of lattice constants and formation enthalpies show close agreement with previously reported theoretical and experimental values for different Fe-Al compounds. The calculated values of formation enthalpies of all Fe-Al compounds were found to be negative, which shows their thermodynamic stability. Calculated elastic constants were found to follow the elastic constant restrictions imposed by the symmetry of the compounds, which further confirms the mechanical stability of the considered Fe-Al compounds. Based on the bulk modulus, FeAl is found to be the hardest and $FeAl_2$ the softest phase. Comparisons of mechanical properties with other theoretical and experimental studies show uncertainties in the calculated values and material properties. However, in general, DFT is found to be in good agreement with most experimental observations.

Declaration of competing interest

The authors declare that they have no known competing financial interests or personal relationships that could have appeared to influence the work reported in this paper.

Appendix

Mechanical stability criteria for Fe-Al compounds are calculated by the following relations [10,53].

Cubic system:

$$(C_{11} - C_{12}) > 0, C_{11} > 0, C_{44} > 0, C_{11} + 2C_{12} > 0 \quad \text{(A.1)}$$

Orthorhombic system:

$$C_{11} + C_{12} + C_{33} + 2C_{12} + 2C_{23} > 0; C_{11} + C_{22} > 2C_{12};$$
$$C_{22} + C_{33} > 2C_{23}; C_{11} + C_{33} > 2C_{13}; C_{ij} > 0 (i = 1 - 6) \quad \text{(A.2)}$$

Monoclinic system:

$$C_{ij} > 0 (ij = 11, 22, 33, 44, 55, 66),$$
$$C_{11} + C_{22} + C_{33} + 2(C_{12} + C_{13} + C_{23} > 0),$$
$$(C_{11}C_{55} - C_{12}^2) > 0, (C_{44}C_{66} - C_{46}^2) > 0, C_{22}C_{33} - C_{23}^2 > 0,$$
$$C_{22}(C_{33}C_{55} - C_{35}^2) + 2C_{23}C_{25}C_{35} - C_{23}^2C_{55} - C_{25}^2C_{33} > 0, \quad \text{(A.3)}$$
$$2[C_{15}C_{25}(C_{33}C_{12} - C_{13}C_{23}) + C_{15}C_{35}(C_{22}C_{13} - C_{12}C_{23})$$
$$+ C_{25}C_{35}(C_{11}C_{23} - C_{12}C_{13})] - [C_{15}^2(C_{11}C_{22} - C_{12}^2)$$
$$+ C_{55}(C_{11}C_{22}C_{33} - C_{11}C_{23}^2 - C_{22}C_{13}^2 - C_{33}C_{12}^2 + C_{12}C_{13}C_{23})] > 0$$

Trigonal system:

$$C_{11} - C_{12} > 0; (C_{11} + C_{12})C_{33} - 2C_{13}^2 > 0;$$
$$(C_{11} - C_{12})C_{44} - 2C_{14}^0 > 0 \tag{A.4}$$

References

[1] A. Hotař, M. Palm, P. Kratochvíl, V. Vodičková, S. Daniš, High-temperature oxidation behaviour of Zr alloyed Fe3Al-type iron aluminide, Corros. Sci. 63 (2012) 71–81.

[2] B.L. Silva, A. Garcia, J.E. Spinelli, The effects of microstructure and intermetallic phases of directionally solidified Al–Fe alloys on microhardness, Mater. Lett. 89 (2012) 291–295.

[3] T. Sakiyama, G. Murayama, Y. Naito, K. Saita, Y.M.H. Oikawa, T. Nose, Dissimilar Metal Joining Technologies for Steel Sheet and Aluminum Alloy Sheet in Auto Body, Nippon Steel Technical Report, Vol. 103, Nippon Steel & Sumitomo Metal Corp., Tokyo, 2013, pp. 91–98.

[4] R. Shull, H. Okamoto, P. Beck, Transition from ferromagnetism to mictomagnetism in Fe–Al alloys, Solid State Commun. 20 (9) (1976) 863–868.

[5] G. Huffman, R. Fisher, Mössbauer studies of ordered and cold-worked Fe–Al alloys containing 30 to 50 at.% aluminum, J. Appl. Phys. 38 (2) (1967) 735–742.

[6] C.-H. Zhang, S. Huang, J. Shen, N.-X. Chen, Structural and mechanical properties of Fe–Al compounds: An atomistic study by EAM simulation, Intermetallics 52 (2014) 86–91.

[7] M.Z. Khalid, J. Friis, P.H. Ninive, K. Marthinsen, A. Strandlie, DFT calculations based insight into bonding character and strength of Fe$_2$Al$_5$ and Fe$_4$Al$_{13}$ intermetallics at Al–Fe joints, Procedia Manuf. 15 (2018) 1407–1415.

[8] E. Lee, B.-J. Lee, Modified embedded-atom method interatomic potential for the Fe–Al system, J. Phys.: Condens. Matter 22 (17) (2010) 175702.

[9] B. Jelinek, S. Groh, M.F. Horstemeyer, J. Houze, S.-G. Kim, G.J. Wagner, A. Moitra, M.I. Baskes, Modified embedded atom method potential for Al, Si, Mg, Cu, and Fe alloys, Phys. Rev. B 85 (24) (2012) 245102.

[10] Y. Liu, X. Chong, Y. Jiang, R. Zhou, J. Feng, Mechanical properties and electronic structures of Fe–Al intermetallic, Physica B 506 (2017) 1–11.

[11] L. Liu, X. Wu, R. Wang, W. Li, Q. Liu, First principle study on the temperature dependent elastic constants, anisotropy, generalized stacking fault energy and dislocation core of NiAl and FeAl, Comput. Mater. Sci. 103 (2015) 116–125.

[12] X.-l. Niu, L.-j. Wang, Effect of transition-metal substitution on electronic and mechanical properties of Fe$_3$Al: First-principles calculations, Comput. Mater. Sci. 53 (1) (2012) 128–132.

[13] M. Mendelev, D. Srolovitz, G. Ackland, S. Han, Effect of Fe segregation on the migration of a non-symmetric Σ5 tilt grain boundary in Al, J. Mater. Res. 20 (1) (2005) 208–218.

[14] B.-J. Lee, M. Baskes, Second nearest-neighbor modified embedded-atom-method potential, Phys. Rev. B 62 (13) (2000) 8564.

[15] B.-J. Lee, M. Baskes, H. Kim, Y.K. Cho, Second nearest-neighbor modified embedded atom method potentials for bcc transition metals, Phys. Rev. B 64 (18) (2001) 184102.

[16] B.-J. Lee, J.-H. Shim, M. Baskes, Semiempirical atomic potentials for the fcc metals Cu, Ag, Au, Ni, Pd, Pt, Al, and Pb based on first and second nearest-neighbor modified embedded atom method, Phys. Rev. B 68 (14) (2003) 144112.

[17] E. Asadi, M.A. Zaeem, S. Nouranian, M.I. Baskes, Two-phase solid–liquid coexistence of Ni, Cu, and Al by molecular dynamics simulations using the modified embedded-atom method, Acta Mater. 86 (2015) 169–181.

[18] E. Asadi, M.A. Zaeem, S. Nouranian, M.I. Baskes, Quantitative modeling of the equilibrium of two-phase solid-liquid Fe by atomistic simulations on diffusive time scales, Phys. Rev. B 91 (2) (2015) 024105.

[19] M. Steinhauser, S. Hiermaier, A review of computational methods in materials science: examples from shock-wave and polymer physics, Int. J. Mol. Sci. 10 (12) (2009) 5135–5216.

[20] M.S. Daw, M.I. Baskes, Embedded-atom method: Derivation and application to impurities, surfaces, and other defects in metals, Phys. Rev. B 29 (12) (1984) 6443.

[21] H. Fang, P.M. Gullett, A. Slepoy, M.F. Horstemeyer, M.I. Baskes, G.J. Wagner, M. Li, Numerical Tools for Atomistic Simulations, Tech. Rep., Sandia National Laboratories, 2004.

[22] M. Baskes, Modified embedded-atom potentials for cubic materials and impurities, Phys. Rev. B 46 (5) (1992) 2727.

[23] B.-J. Lee, A modified embedded-atom method interatomic potential for the Fe–C system, Acta Mater. 54 (3) (2006) 701–711.

[24] J. Schneider, J. Hamaekers, S.T. Chill, S. Smidstrup, J. Bulin, R. Thesen, A. Blom, K. Stokbro, ATK-ForceField: a new generation molecular dynamics software package, Modelling Simulation Mater. Sci. Eng. 25 (8) (2017) 085007.

[25] Atomistix Toolkit version 2017.0, Synopsys QuantumWise A/S, www.quantumwise.com.

[26] J. Nocedal, Updating quasi-Newton matrices with limited storage, Math. Comp. 35 (151) (1980) 773–782.

[27] W. Voigt, Lehrbuch der kristallphysik (mit ausschluss der kristalloptik), Springer-Verlag, 2014.

[28] A. Reuss, Berechnung der fließgrenze von mischkristallen auf grund der plastizitätsbedingung für einkristalle, ZAMM Z. Angew. Math. Mech. 9 (1) (1929) 49–58.

[29] R. Hill, Proc. Phys. Soc. Lond. A (1952).

[30] Н. Н Лякишев, Handbook of Binary Alloy Phase Diagrams, Beijing Chemical Industry Press, Beijing, China, 2009.

[31] P.G. Gonzales-Ormeño, H.M. Petrilli, C.G. Schön, Ab-initio calculations of the formation energies of BCC-based superlattices in the Fe–Al system, CALPHAD 26 (4) (2002) 573–582.

[32] W. Pearson, WB Pearson: A Handbook of Lattice Spacings and Structures of Metals and Alloys, Pergamon Press, London, New York, Paris, Los Angeles, 1958, p. 1044, 13 (8) (1958) 516.

[33] C. Vailhe, D. Farkas, Shear faults and dislocation core structure simulations in B2 FeAl, Acta Mater. 45 (11) (1997) 4463–4473.

[34] P.D. Desai, Thermodynamic properties of selected binary aluminum alloy systems, J. Phys. Chem. Ref. Data 16 (1) (1987) 109–124.

[35] E.A. Brandes, G. Brook, Smithells Metals Reference Book, Elsevier, 2013.

[36] P. Villars, Pearson's Handbook—Desk Edition: Crystallographic Data for Intermetallic Phases, ASM International, Materials Park, OH, 1998, pp. 1727–1729.

[37] R. Hultgren, P.D. Desai, D.T. Hawkins, M. Gleiser, K.K. Kelley, Selected Values of the Thermodynamic Properties of Binary Alloys, Tech. Rep., National Standard Reference Data System, 1973.

[38] Y. Ouyang, X. Tong, C. Li, H. Chen, X. Tao, T. Hickel, Y. Du, Thermodynamic and physical properties of FeAl and Fe$_3$Al: an atomistic study by EAM simulation, Physica B 407 (23) (2012) 4530–4536.

[39] G. Simmons, H. Wang, et al., Single Crystal Elastic Constants and Calculated Aggregate Properties, MIT Press, Mass, 1971.

[40] G. Zhang, M. Chen, Y. Shi, J. Huang, F. Yang, Analysis and modeling of the growth of intermetallic compounds in aluminum–steel joints, RSC Adv. 7 (60) (2017) 37797–37805.

[41] H. Titrian, U. Aydin, M. Friák, D. Ma, D. Raabe, J. Neugebauer, Self-consistent scale-bridging approach to compute the elasticity of multi-phase polycrystalline materials, in: MRS Proc, Vol. 1524, 2013.

[42] M. Friák, W.A. Counts, D. Ma, B. Sander, D. Holec, D. Raabe, J. Neugebauer, Theory-guided materials design of multi-phase Ti-Nb alloys with bone-matching elastic properties, Materials 5 (10) (2012) 1853–1872.

[43] L.-F. Zhu, M. Friák, L. Lymperakis, H. Titrian, U. Aydin, A.M. Janus, H.-O. Fabritius, A. Ziegler, S. Nikolov, P. Hemzalová, et al., Ab initio study of single-crystalline and polycrystalline elastic properties of Mg-substituted calcite crystals, J. Mech. Behav. Biomed. Mater. 20 (2013) 296–304.

[44] L. Sun, Y. Gao, B. Xiao, Y. Li, G. Wang, Anisotropic elastic and thermal properties of titanium borides by first-principles calculations, J. Alloys Compd. 579 (2013) 457–467.

[45] J. Haines, J. Leger, G. Bocquillon, Synthesis and design of superhard materials, Annu. Rev. Mater. Res. 31 (1) (2001) 1–23.

[46] W.H. Wang, Correlations between elastic moduli and properties in bulk metallic glasses, J. Appl. Phys. 99 (9) (2006) 093506.

[47] H.-Y. Chung, M.B. Weinberger, J.-M. Yang, S.H. Tolbert, R.B. Kaner, Correlation between hardness and elastic moduli of the ultraincompressible transition metal diborides Ru B 2, Os B 2, and Re B 2, Appl. Phys. Lett. 92 (26) (2008) 261904.

[48] J. Schroers, W.L. Johnson, Ductile bulk metallic glass, Phys. Rev. Lett. 93 (25) (2004) 255506.

[49] K. Gschneidner Jr., A. Russell, A. Pecharsky, J. Morris, Z. Zhang, T. Lograsso, D. Hsu, C.C. Lo, Y. Ye, A. Slager, et al., A family of ductile intermetallic compounds, Nature Mater. 2 (9) (2003) 587.

[50] S. Pugh, XCII. Relations between the elastic moduli and the plastic properties of polycrystalline pure metals, Lond. Edinb. Dublin Phil. Mag. J. Sci. 45 (367) (1954) 823–843.

[51] L. Tricarico, R. Spina, D. Sorgente, M. Brandizzi, Effects of heat treatments on mechanical properties of Fe/Al explosion-welded structural transition joints, Mater. Des. 30 (7) (2009) 2693–2700.

[52] S. Bozzi, A. Helbert-Etter, T. Baudin, B. Criqui, J. Kerbiguet, Intermetallic compounds in Al 6016/IF-steel friction stir spot welds, Mater. Sci. Eng. A 527 (16–17) (2010) 4505–4509.

[53] F. Mouhat, F.-X. Coudert, Necessary and sufficient elastic stability conditions in various crystal systems, Phys. Rev. B 90 (2014) 224104, http://dx.doi.org/10.1103/PhysRevB.90.224104, URL https://link.aps.org/doi/10.1103/PhysRevB.90.224104.